

## Tools

Friedrich Wiegel\*, Jan Wachter, Michael Kyesswa, Ralf Mikut, Simon Waczowicz and Veit Hagenmeyer

# Smart Energy System Control Laboratory – a fully-automated and user-oriented research infrastructure for controlling and operating smart energy systems

Smart Energy System Control Laboratory – hochgradig automatisierte und nutzerorientierte Forschungsinfrastruktur zur Steuerung und zum Betrieb intelligenter Energiesysteme

<https://doi.org/10.1515/auto-2022-0018>

Received February 14, 2022; accepted October 16, 2022

**Abstract:** In the present paper, we introduce the Smart Energy System Control Laboratory (SESCL) as a fully-automated and user-oriented research infrastructure for controlling and operating smart energy systems in the context of a microgrid-under-test setting. SESCL's high level of automation and capacity to fully function in a grid-decoupled way allow for the study and evaluation of yet-to-be-developed tools and algorithms for energy technologies and grid control strategies on the edge of system stability, but in a safe environment. In the context of various European Smart Grid Laboratories, the new concept and specifications of SESCL are outlined in depth. The key advantages of SESCL are highlighted as (i) the provisioning of a fully-automated busbar matrix to provide a very flexible and adjustable microgrid topology; (ii) the capability of load shedding or integration of grid participants, as well as changing the microgrid topology

**Dedicated to:** We dedicate the present article to Dr. Jörg Isele, who, as head of the research area Research Platform Energy, was the mastermind behind the planning and construction of the Smart Energy System Control Laboratory. Jörg Isele passed away on August 19, 2019.

**\*Corresponding author: Friedrich Wiegel**, Karlsruhe Institute of Technology, Institute for Automation and Applied Informatics, Eggenstein-Leopoldshafen, Germany, E-mail: [friedrich.wiegel@kit.edu](mailto:friedrich.wiegel@kit.edu). <https://orcid.org/0000-0001-6984-7208>

**Jan Wachter, Michael Kyesswa, Ralf Mikut, Simon Waczowicz and Veit Hagenmeyer**, Karlsruhe Institute of Technology, Institute for Automation and Applied Informatics, Eggenstein-Leopoldshafen, Germany

on demand; (iii) and the possibility to control and modify setpoints and operating parameters of grid participants during runtime. Inspired by real-world events in island grids, the islanding of a microgrid is utilized as a use case to illustrate the capabilities of the SESCL research infrastructure.

**Keywords:** control and automation in microgrids and smart grids; islanding of a microgrids; large scale research infrastructure; microgrid-under-test; power-hardware-in-the-loop.

## 1 Introduction

The reliable, affordable and sustainable energy supply of the future will be largely achieved by the efficient conversion of primary renewable energy sources into secondary energy sources, such as electricity, heat and fuels. Recent studies show that energy systems based on renewables are feasible, economically viable and decrease in cost every year [1, 2]. Thereby, the electricity sector plays a key role since it offers reliable, proven and robust generation technologies from renewable energy sources (RES), such as wind power plants and photovoltaic systems.

The transition of the electric power supply to exclusively renewable, decentralized and fluctuating energy sources entails risks with regard to the energy trilemma of security of supply, economic viability and environmental pollution [3]. Security of supply becomes even more challenging, as the number of fossil base load power plants will have to be massively reduced to ensure an environmentally friendly energy supply. In turn, the respective rotating masses representing the inertia in the actual system for

the spinning reserve are withdrawn from the system, increasing the risk of a large-scale system blackout [4].

The challenges which power grids are facing as a result of this inevitable transformation are: (i) Conversion of demand-driven power generation into weather-dependent and production-driven generation due to an increasing penetration of wind power plants and photovoltaic systems [5, 6]. (ii) While the current flow used to be top-down, i.e. from high to low voltage levels, there are more bottom-up flows from lower voltage levels to the higher ones as a result of decentralized generation. (iii) In addition to the developments on the generation side, the consumption characteristics will also change: The grid integration of battery electric vehicles, electrification of heating systems and other consumers will bring even greater momentum into the distribution network and burden it additionally due to unpredictable high peak loads with steep gradients. (iv) Due to substantial quantities of volatile energies in both production and consumption as well as massive decentralization of production sites, classical grid control approaches are no longer appropriate [7].

Consequently, this leads to fundamental changes in the design and operation of power systems. A modern power grid managed and operated on the basis of smart grid and microgrid concepts is a key enabler for ensuring a reliable and sustainable power supply [8]. In combination with information and communication technologies (ICT), intelligent electronic devices (IED) and advanced automation systems, these concepts form a solid foundation for the stable, effective and economical operation of future power grids [9–11].

Research activities carried out by academia provide an important contribution, e.g. through architectural concepts and system-level developments. However, concepts on grid operation cannot be based solely on theoretical and simulative considerations alone. Validation and testing plays a significantly role in realizing future solutions and technologies [9, 12]. In this context, new grid control and automation concepts as well as power system developments cannot be tested in the public grid due to the risk of a blackout [13]. Hence, there is a need for experimental microgrid facilities in the power range of several hundred kilowatts – in accordance with real island grids [14] – where ideas may be put to the test in real-world settings, providing experimental proof of the novel solutions and thus increasing the attractiveness for stakeholders [15, 16]. In addition, empirical evidence shows that many of the phenomena occurring in real-world processes do not occur in stand-alone testbench settings and are readily neglected in simulations as well.

With the Energy Lab 2.0,<sup>1</sup> the Helmholtz Association is realizing a large scale replication of the current and future energy system that contains all relevant process chains for generation, conversion and storage of various energy sources. The scope of the Energy Lab 2.0 is to develop technological solutions for the overall future energy system in order to successfully integrate renewable energies into the power grid, particularly by conducting technology-oriented research on a demonstrator scale and supplementing it with comprehensive energy systems analysis [17].

The Smart Energy System Control Laboratory (SESCL) represents an essential part of the Energy Lab 2.0. SESCL provides a fully-automated and user-oriented research infrastructure with a topology-adjustable microgrid. The goal of SESCL is to model, control and experimentally validate new energy technologies. Since the laboratory can be operated decoupled from the public grid, grid control strategies can be studied and evaluated in regions of critical stability [18] without the risk of large-scale blackouts. The research topics within the scope of SESCL include

- control and automation in microgrids and smart grids,
- the integration of distributed energy resources (DERs),
- system stability analysis of converter dominated alternating current (AC) and direct current (DC) microgrids,
- the interplay between microgrid and macrogrid in the two modes “grid-connected” and “island” and the transition between the two modes,
- new operation concepts of microgrids and smart grids,
- and energy conversion in smart grids.

The main contributions of the present article are:

1. A brief overview of smart grid research infrastructures that have similar equipment and research orientation, followed by a discussion of the major features in which SESCL differs from them (Section 2).
2. A detailed description of the fully-automated and user-oriented concept, benefits, and specifics, including the provision of a unique setting for microgrid-under-test (MUT) as a power-hardware-in-the-loop (PHIL) service by the Smart Energy System Control Laboratory (Section 3). The description is aimed specifically at potential users of the research infrastructure.
3. The presentation of a use case to demonstrate the capabilities of the SESCL research infrastructure (Section 4).

<sup>1</sup> [www.elab2.kit.edu/english/index.php](http://www.elab2.kit.edu/english/index.php).

Section 5 closes the present article giving relevant conclusions and an outlook for future collaboration.

## 2 Related work

Driven by the urgent need for action in the field of smart and sustainable energy systems identified by society and governments, numerous test labs for smart energy systems similar to SESCL, respectively Energy Lab 2.0, have been applied in recent years. The report “Smart Grid Laboratory Inventory” and the survey “Smart grid lab research in Europe and beyond” published by the European Commission, Joint Research Centre (JRC) provide a comprehensive overview of the laboratories in this research area worldwide [19, 20]. The key messages of the two essays are that 77% of the laboratories are located in Europe – this can be explained by the high funding budget provided by the European Union -, the laboratories are often active in a multitude of research areas of smart energy systems and that the increasing research trend in this area continues. The number of research facilities in the smart energy systems research area is between 75 and 89 according to our literature review. The variation in the number depends on whether facilities under construction (planned) are counted. However, since the focus and main research activities of the individual institutions differ, a direct comparison would only be moderately meaningful. Nevertheless, based on publicly available information on the equipment and profiles of selected facilities, an attempt is made to identify research trends in the field of smart energy systems.

The Smart Electricity Systems and Technologies (SmartEST) laboratory at the Austrian Institute of Technology provides three independent three-phase low voltage busbars with adjustable loads for active and reactive power, two grid simulators with up to 480 V and 850 kVA. SmartEST also has several DC sources for dynamic simulation of PV systems and is able to carry out real-time simulation and (power-) hardware-in-the-loop (PHIL respectively HIL) experiments using OPAL-RT real-time simulators [21]. In addition, the climate test chamber enables validation and testing of power system components under extreme temperature and humidity conditions. According to the information on the ERIGrid 2.0<sup>2</sup> homepage, the laboratory is equipped with a customizable supervisory control and data acquisition (SCADA) and automation system which unfortunately is not specified

further. The research activities of the laboratory are in the integration of power converter driven systems, grid simulation and management as well as data analytics.

Norwegian University of Science and Technology (NTNU) and SINTEF jointly operate the Norwegian National Smart Grids Laboratory as a smart energy systems experimental facility. The research covers transmission and distribution grids, microgrids, integration of renewables, energy storage and conversion as well as big data management and analytics in smart energy systems. The laboratory is equipped with state-of-the-art physical assets with ratings up to 200 kVA, 400 V AC or 700 V DC strongly similar to those at SESCL, including various renewable sources, transmission systems, electric vehicle charging stations, AC/DC converters, electric motors, OPAL-RT real-time simulator and Egston power amplifier [22, 23].

Smart Grid Technology Lab at the Technical University Dortmund has a low voltage grid with several adjustable lines, energy storage systems, PV system emulator, transformers with on-load tap changers, controllable loads, electrical vehicle charging stations, line voltage regulators and PHIL equipment. The PHIL equipment includes an OPAL-RT OP5607 real-time simulator and an 200 kVA Egston power amplifier. One of the laboratory’s unique features is the data stream provided by various distribution system operators [24].

PREDIS is Grenoble-INP’s smart grid platform that works closely together with Grenoble Electrical Engineering Laboratory (G2ELab). PREDIS reconfigurable electrical grid provides reduced scale (20 kV–400 V and 30 MVA to 30 kVA) flexible electrical grids of the French medium voltage (MV) grid. It includes 14 nodes, several loads and generators in the range up to 30 kVA. The model grids are intended to represent a 30 MVA total consumption and 27.25 MW of total generation in scale 1:1000. In addition, the laboratory is equipped with an appropriate SCADA system and PHIL facilities. The main activity of the laboratory is research in the field of smart grids and technology transfer to industry [25, 26].

With the Smart Energy System Laboratory at Aalborg University, a platform was created that connects smart energy system demonstrators, real-time hardware-in-the-loop platforms, and distributed energy resources that were already present at the university. It includes a 50 kVA four-quadrant grid simulator, 20 kW/10 kVAr four-quadrant emulator for dispersed generation, PV emulator, energy storage system, various programmable AC loads, digital real-time simulators as well as appropriate SCADA and monitoring system [27].

<sup>2</sup> www.erigrd2.eu.

A number of similar research facilities in the field of smart energy systems are also operated, for example, by Électricité de France (EDF), National Renewable Energy Laboratory (NREL), TU Delft and other institutions [19, 20]. In general, the equipment – possibly differentiated by performance classes – as well as the research activities and instrumentation are similar at most facilities. Also, all laboratories ensure that experiments can be carried out in a safe environment.

A close examination of publicly available data, published articles, and press releases on competitor facilities reveals that for reasons of personal and equipment protection, most of the laboratories for smart energy technical systems presented in the paper may only be operated by designated personal or specialists with a high degree of facility as well as energy technology prior knowledge. This is usually due to the lack of automated preliminary conformity checks of the test setup and experiment procedure, as well as permanent machine-aided supervision of the entire test field, which, in the worst-case scenario, would reliably and safely clear the error case without the operator's intervention. As a result, non-facility-experienced and non-field-tested theoretical researchers face a higher barrier to entry into the laboratory application. Consequently, this is reflected in the resulting low number of genuine testing of novel and promising control concepts developed in the context of theoretical research.

In addition, the presented facilities' instrumentation solutions lack the concept of legitimate generalization or abstraction of device-specific functions across an environment, as envisioned by IEC 61850 [28]. The definition and usage of globally valid abstract properties increases the user-friendliness through recognition value and reduction of plant-specific functions, which enables the interchangeability of the equipment without intervening in the overall instrumentation architecture of the facility and brings advantages in the (preliminary) modeling and post-analysis of the experiment.

Moreover, through the literature review, it can be identified that the electrical connections between the resources within the test facilities allow a relatively low degree of freedom in terms of topology variation of the available test grid without time-consuming and costly manual intervention by the laboratory personnel.

In turn, SESCL also represents a large-scale test and validation infrastructure for smart energy systems and grids, which allows experiments to be performed safely, but almost independently of the user's experience in a very user-friendly manner. The experimental facility's safety is ensured by the advanced automation system, since the

permissibility of the connection is automatically checked beforehand and during runtime as well as by using the fully-automated busbar matrix to provide the grid topology in a way that no manual work is required on electrical components. The system design allows easy realization of load shedding or integration of additional generators, consumers or prosumers during runtime and changing the grid topology on demand. Another key aspect of the automation system is that it allows up to four experiments in parallel with a fully-automated resource allocation corresponding to the user authorization. Furthermore, the automation system monitors and controls the busbar matrix itself, the individual components as well as the schedule of a planned experiment. Besides ensuring safe operation, aspects like (i) fast system access; (ii) comprehensive user and resource management; (iii) user-friendly planning, execution and monitoring of experiments; and (iv) repeatability of experiments play a crucial role in the system design.

Finally, many of the smart grid labs mentioned above lack detailed documentation of the research infrastructure in terms of hardware and software and its practical use. To the best of our knowledge, there are only few scientific publications that describe in detail the hardware (design of circuits and built-in protection measures, integrated EMC solutions, etc.) and information architecture (automation system, information and communication technology) structure of a smart grid laboratory [26, 27, 29]. Inspired by the open-source approach, this contribution strives to provide a holistic open-solution guide for establishing fully-automated and user-oriented test facilities for energy systems.

## 3 Smart Energy System Control Laboratory

### 3.1 Concept

To provide realistic low voltage grids for experiments, the laboratory includes a variety of energy technology system components, such as generators, converters, inverters, photovoltaic system (PV), battery energy storage systems (BESS), smart houses etc. The components can be freely interconnected – in terms of topology – while taking into account the physical transmission line characteristics to form a microgrid with variable topology. The connection flexibility is ensured by the heart of the laboratory: a matrix of ten busbars and 424 contactors controlled by a central automation system, cf. Figure 1. With respect to

the operating mode, the busbar matrix can be divided into two segments: AC and DC. The AC part consists of eight three-phase TN-C-S system busbars of the low voltage level (horizontal lines). To interconnect the busbars while taking into account the transmission behavior of cables or overhead lines, the laboratory has both real transmission lines and line replicas that use discrete RLC components – in  $\pi$ -type topology – to represent the physical behavior of a transmission line of variable length (cf. Figure 1). A total of 71 grid participants (59 AC grid participants and 12 DC grid participants) can be connected to the busbars via an arrangement of contactors (cf. Figure 1 red diamonds). The connection points of the participants are represented in Figure 1 as columns to the busbars. This creates the matrix shown in Figure 1. The differently sized diamonds symbolize different contactor performance classes. By design, power systems of the following ratings 400 A, 125 A, 63 A, 32 A and 16 A can be connected to the matrix.

The DC segment of the matrix is constructed identically in terms of logical structure and operation. It has two two-pole busbars that can be connected to each other via a line replica. Up to twelve components can be interconnected to the DC grid with variable topology. It is designed for an operating voltage of 700 V and a current up to 220 A.

Such a complex electrical system is brought to life by means of an appropriate and comprehensive automation system. It monitors and controls both the entire system and the individual components as well as the schedule of the experiment. It is responsible for the acquisition, visualization and logging of all experimental, plant-relevant and component-specific measured variables such as current, voltage, network frequency, power, harmonics, etc. The

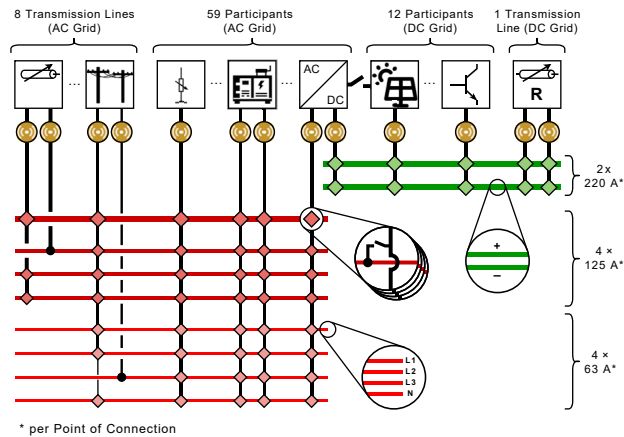


Figure 1: Structure of the busbar matrix.

acquisition of the measured variables is undertaken in the AC domain with 20 kHz and in the DC domain with 100 kHz. In addition, information about the user, approved resources, used source code etc. is archived. Via a graphical interface, a user can easily select the resources approved for him and integrate the resource into a topology of his planned experiment. Up to four experiments can be run in parallel and can be monitored in real-time by the laboratory management via the process control center.

OPAL-RT real-time simulation systems as well as two Egston power-hardware-in-the-loop (PHIL) amplifiers with up to eight channels and a total power of 200 kVA as well as several power electronics testbench systems from Imperix for power converter rapid prototyping complete the hardware equipment of the laboratory.

As a result, an overall concept with a high degree of integration of various disciplines is developed, as shown in Figure 2, that enables smooth planning, execution, recording as well as evaluation and repetition of an experiment. In the following, the role of the individual elements depicted in Figure 2 is discussed in more detail.

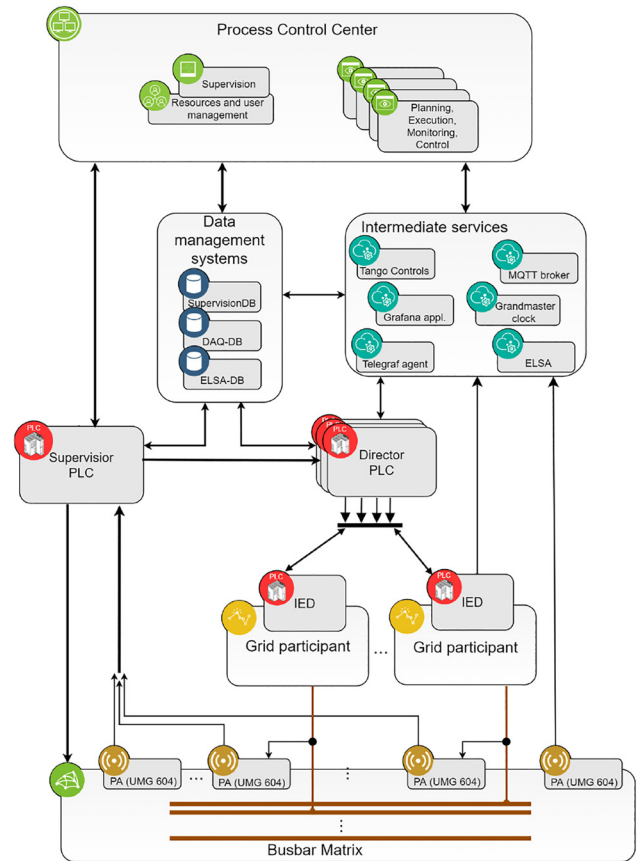


Figure 2: Automation and IT architecture.

### 3.2 Hardware components

#### 3.2.1 Electrical circuits

In order to avoid undesired interferences and to ensure an uninterruptible power supply (UPS) of the building, and the measurement and control equipment, different circuits have been implemented in the lab building as shown in Figure 3 and can be classified as follows:

- (i) The facility supply is provided via transformer T1. Measurement equipment, servers, clients, programmable logic controllers (PLCs) and other equipment that must operate at least temporarily in the case of a blackout in order to record the processes and bring the components into a controlled state are fed from this circuit via an UPS.
- (ii) Transformer T2 provides a 0.4 kV low voltage grid for the power supply of the experimental field. It is used to supply the PHIL systems, motor-generator sets (M-G sets) and other components that are feed-back capable.
- (iii) The actual object of investigation is one or more island grid – highlighted in red in Figure 3 – formed by the busbar matrix and the corresponding components including the transmission lines. The experimental grid is formed e.g. by a M-G set, PHIL system or a grid-forming converter. Other producers feed synchronously into the island grid.
- (iv) Additionally, the so-called PHIL Laboratory<sup>3</sup> operates a PHIL system with a total power of 1 MVA which

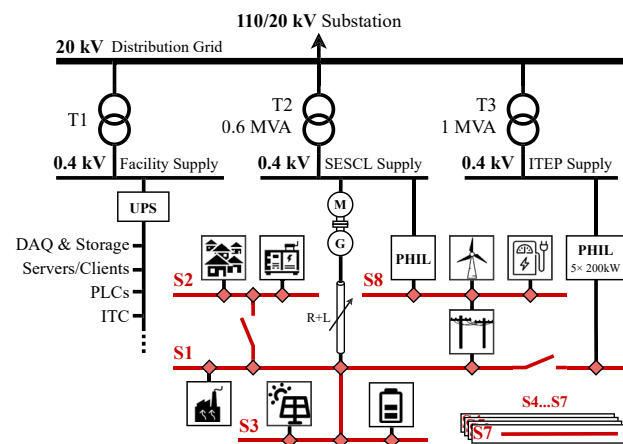


Figure 3: Schematic of electrical circuits in the lab building.

is fed by a separate transformer T3. This PHIL system can also be integrated into the experimental grid, however with a power limitation.

#### 3.2.2 Busbar matrix

Figure 4 shows the concept and the simplified structure of the cabinet for the first four busbars of the AC segment. Busbars S5 to S8 are an extension of this concept. This cabinet allows connecting up to four grid participants to the matrix. The whole matrix is formed by 32 analog cabinets. The DC section is implemented following to a similar idea, with the corresponding specifications and safety requirements.

For the dimension of the busbars, a preliminary estimation was carried out. This resulted in a possible continuous current of 550 A per phase and short-circuit currents smaller than 10 kA. To ensure the conceptual reserve, the busbars were designed for a continuous current of 800 A per phase and a short-circuit strength of 50 kA. Furthermore, all contactors within the matrix (i) are designed as all-pole switchable to ensure safe disconnection of the loads and (ii) are of different device categories to be able to switch different load types (resistive, capacitive and inductive) safely even under load. The control voltage of the contactor coils is carried out via a separate circuit than that of the PLC and the measuring system supply in order to avoid an undesired interference.

The overall protection concept is ensured by the automation system based on preliminary verification of

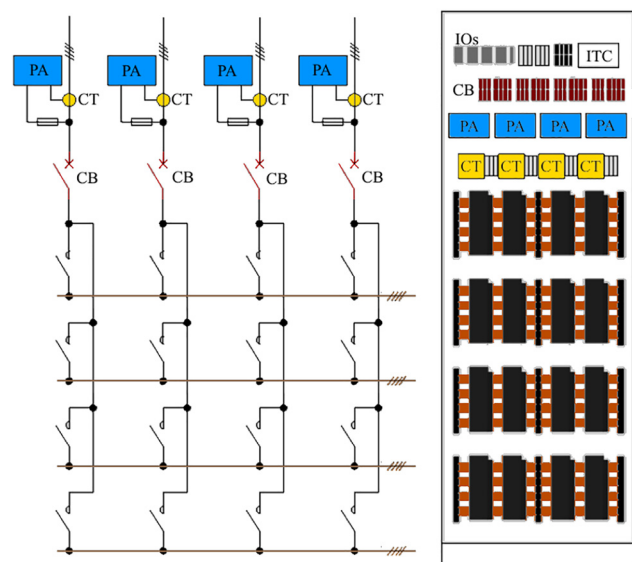


Figure 4: Concept and structure of a busbar matrix cabinet.

the experiment, the measured values during the execution of the experiment, and the device safety measures of the respective grid participant. In addition, the plant and experimental field safety is ensured by thermal-magnetic and thermal circuit breakers on each point of connection to the busbar matrix. Potential shorts of the contactor switching states are prevented both by the automation system and by mutual hardware interlocking.

### 3.2.3 Measurement equipment

Field measurement equipment can be divided into three categories: (i) test measurement equipment, (ii) component measurement equipment, and (iii) system measurement equipment. Test measurement equipment are portable, high-precision measurement devices used for reference measurement and calibration. They enable the acquisition of specific measured values during an explicit experiment at a defined measuring point according to a specific research question. Component measurement equipment are measurement devices installed inside of the grid participants and explicitly adjusted to the respective requirements, e.g. 4Q Smart Meter or  $\mu$ PMU. The system measurement equipment are Power Analyzer UMG 604-PRO from Janitza. They are installed on each branch of the matrix and record voltages and currents – as well as derived values such as power, frequency etc. – on all four conductors ( $3p + n$ ), cf. Figure 4. The main specifications of the power analyzers are summarized in Table 1.

The power analyzers are equipped with two independent interfaces – Ethernet and RS-485 – as well as custom firmware. Through the RS-485 interface, the power analyzers are integrated into the supervision task of the automation system via Modbus-RTU. Using this interface, relevant root mean square (RMS) values with a time resolution of 1 s are provided to ensure the safe operation of the lab. These are used for: live display of critical system parameters during test runs on the operator panel; checking the total authorized power per user; and calculating the total currents per busbar to trigger software trips in order to prevent system overload.

Two further services are provided via the Ethernet interface. By means of HTTPs requests of the Telegraf<sup>4</sup> server agent, the energy-related parameters calculated by the internal digital signal processor (DSP) are made available as live value dashboards as well as stored in the time series database – specifically InfluxDB<sup>5</sup> – for

**Table 1:** Specifications of Janitza power analyzer UMG 604-PRO.

Parameter	Value
Voltage range L-N(L)	0 to 600 (1000) Vrms
Voltage resolution	0.01 V
Impedance measurement	4 M $\Omega$ /phase
Current range	CT dependent
Current resolution	10 mA (or resolution of CT)
Sampling rate	20 kHz
Frequency metering range	45 Hz–65 Hz
Frequency/phase resolution	1 mHz/0.15°
Clock synchronization	PTP and NTP

permanent data recording and subsequent analysis. The time resolution of these values is 200 ms.

The combination of a custom firmware and the Energy Lab Signal & Analyze (ELSA) intermediate service – cf. Section 3.3 – completes the function of the power analyzer as a system measurement device. The customized firmware allows access to the raw data ( $U$  and  $I$ ) directly after the antialiasing filter of the UMG 604-PRO. These raw data, which are stored in a ring buffer with a time resolution of 50  $\mu$ s and 10 mV/10 mA, are collected, compressed and stored in TimescaleDB by ELSA. Moreover, ELSA makes the logged values available via a web application both as live values and as waveforms over a specified time period.

### 3.2.4 Grid participants

The laboratory has a wide range of low voltage distribution grid components. Among these are synchronous generators, emergency power systems, renewable energy sources such as photovoltaic systems, wind power plants and geothermal power plants, chemical and kinetic energy storage systems, distribution transformers with on-load tap changer (OLTC), transmission line replica as well as active and passive controllable RLC loads. Furthermore, the model houses of the Living Lab Energy Campus<sup>6</sup> and a charging station including vehicle-to-grid (V2G) capable vehicles are integrated into the laboratory via the matrix. A detailed list of the available components and their characteristics can be found on the SESCL Homepage.<sup>7</sup> In addition, a virtual lab tour<sup>8</sup> of the laboratory was developed.

<sup>4</sup> [www.influxdata.com/time-series-platform/telegraf](http://www.influxdata.com/time-series-platform/telegraf).

<sup>5</sup> [www.influxdata.com](http://www.influxdata.com).

<sup>6</sup> [www.iai.kit.edu/english/RPE-LLEC.php](http://www.iai.kit.edu/english/RPE-LLEC.php).

<sup>7</sup> [www.iai.kit.edu/english/RPE-SESCL.php](http://www.iai.kit.edu/english/RPE-SESCL.php).

<sup>8</sup> <https://panorama.cloud.iai.kit.edu>.

**M–G set:** A major grid participant of the laboratory is the motor-generator set with a flywheel coupled via a V-belt. This set can be operated both as a grid forming system with an adjustable nominal frequency as part of an island grid and in grid parallel mode with the option of automated synchronization and connection. The flywheel makes it possible to realistically reproduce the behavior of a conventional power plant, e.g. gas turbine power plant, in the performance class of the experimental field. The installed flywheel mass was designed according to the following estimation:

For the year 2035 a maximum power generation of  $P_0 = 150$  GW and a maximum load step of  $P_\Delta = 3$  GW, corresponding to 2%, is assumed according to the study of German Energy Agency [30]. The system inertia needs to be available for the duration of the ramp up time  $\tau_{AN} = 10 \dots 12$  s and should prevent the maximum permissible frequency deviation of 0.2 Hz from being exceeded. Thus, the flywheel needs to provide 2% of the system power for about 10 s while reducing the speed from 3000 rpm ( $f_1 = 50$  Hz) to at least 2988 rpm ( $f_2 = 49,8$  Hz).

Due to its design, the M–G set has a certain moment of inertia. This has to be increased by adding an additional mass such that  $\Delta W_{ROT} = 0.02W_{ROT}$ . For a  $S_0 = 40$  kVA machine this corresponds to a work of:

$$\Delta W_{ROT} = \frac{P_\Delta}{P_0} \cdot S_0 \cdot \tau_{AN} = 8 \text{ kWs} \quad (1)$$

The required moment of inertia is given by:

$$J = \frac{2 \cdot \Delta W_{ROT}}{\omega_1^2 - \omega_2^2} = 20.3 \text{ kgm}^2 \quad (2)$$

with  $\omega_1 = 2\pi f_1$  and  $\omega_2 = 2\pi f_2$ . The mass of the flywheel with the fixed radius  $r = 320$  mm is therefore:

$$m = \frac{2 \cdot J}{r^2} = 396.5 \text{ kg} \quad (3)$$

By construction, the pulleys on the generator shaft and the flywheel are exchangeable. This allows to vary the transmission ratio between the generator and the flywheel in a certain range. Thus, both the ratio  $\frac{P_\Delta}{P_0}$  and  $\tau_{AN}$  can be varied according to the requirements. Besides providing system inertia the M–G set can be used in grid parallel operation for power factor correction.

**PHIL:** Naturally, the laboratory’s resources are finite. Devices that do not exist physically in the lab can be represented by PHIL systems [31]. Figure 5 illustrates the concept of a PHIL simulation based on a typical SESCL application. The objective of the study is to analyze the effects of various control concepts of the feed-in power of a wind turbine on a microgrid with small control reserve. The basic condition is: A wind turbine is not available, but a sufficiently accurate model of the wind turbine is present. The behavior of the microgrid to be investigated (and the grid participants) is not known due to the volatile grid participants, but the microgrid to be investigated is physically accessible. For the analysis, the wind turbine is simulated on a real-time simulator and connected to the “real” microgrid via a power amplifier. From the perspective of the microgrid, a real wind turbine is associated with its typical behavior, or rather the behavior desired by the researcher, despite the fact that the behavior is only emulated by power amplifiers that are controlled by a corresponding output signal from the real-time simulator. Conversely, the simulation system running the wind turbine model receives a feedback signal from the microgrid (typically current or voltage) that reflects the effect of the wind turbine’s behavior on the real microgrid. This feedback signal or its constituents are fed to the control algorithms of the wind turbine model, thus closing the loop of the PHIL simulation as defined.

Of course, PHIL simulation can be used to simulate not only devices but also grids or grid sectors, which are then

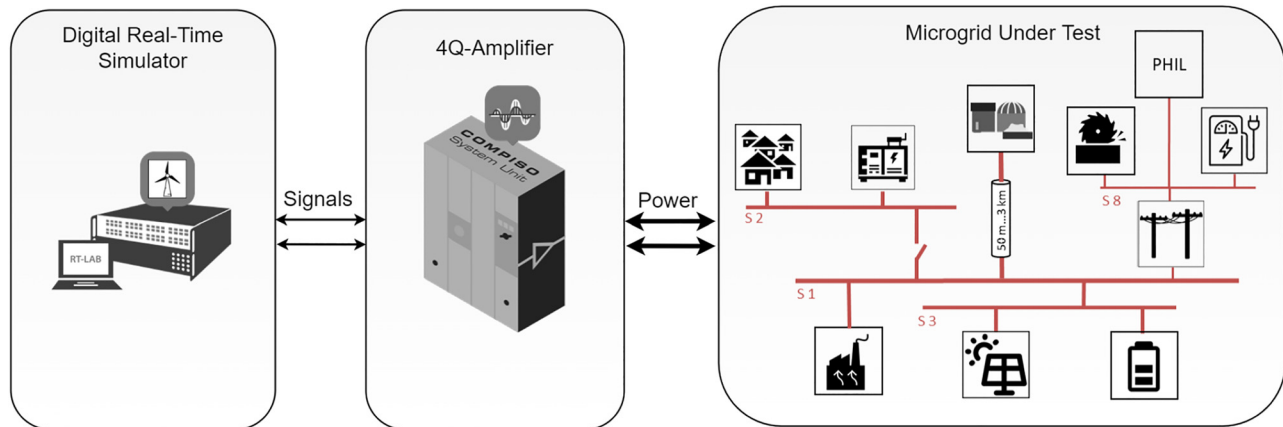


**Figure 5:** A schematic illustration of a power-hardware-in-the-loop simulation system setup.



connected via power amplifiers to the SESCL microgrid at the point of common coupling. The lab's diverse PHIL equipment includes two CSU100 2GAMP4 four-quadrant amplifiers from Egston, two OP5707 real-time simulators with ten real-time simulation cores each, two OP4510 with two real-time simulation cores each as well as an OP1420 microgrid testbench from OPAL-RT. Moreover, the 1 MVA PHIL system can be coupled to the test field via the matrix.

**TRL:** Transmission lines (TRLs) and their replicas are further key elements of the lab. As already mentioned, they allow to connect the busbars with each other, while taking into account the transmission behavior of cables or overhead lines, and thus providing different grid sections. Besides real transmission lines of constant length, line replicas composed of discrete RLC components in  $\pi$ -topology are used in SESCL to represent the physical behavior of a transmission line with variable length. A total line length of approx. 3 km can be realized in increments of 10 m–100 m, depending on the type of cable to be simulated. This corresponds to primary line constants with the sizes of 22 m $\Omega$  – 1.6  $\Omega$  for resistance, 1.1–562.1  $\mu$ H for inductance and 2–1024 nF for capacitance each with an increment of  $\Delta R = 3.125$  m $\Omega$ ,  $\Delta L = 1.1$   $\mu$ H and  $\Delta C = 2$  nF. The replication of a line is done by selectively switching resistive and inductive load units in a serial (RL part) or capacitive load units in a parallel (C part) arrangement.

As expected, the measurements taken during initial deployment showed that parasitic effects of the RL components cannot be neglected and result in significant deviations from nominal values, cf. Figure 6. Thus, the  $R$  and  $L$  components cannot be controlled individually, but are handled as a combinatorial set. The resulting total resistance and inductance values  $R_i$  and  $L_i$  of the line replica are dependent on the switching states  $i$  and can be described mathematically by:

$$\begin{aligned} R_i &= R(i) + R_L(i) + R_0 \\ L_i &= L(i) + L_R(i) + L_0 \end{aligned} \quad (4)$$

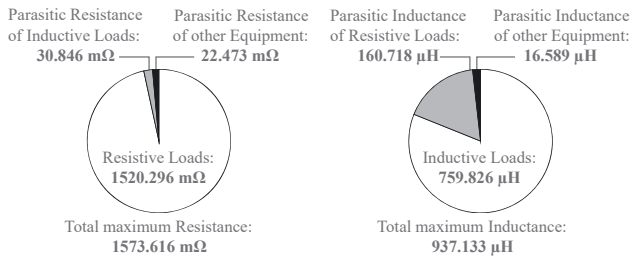


Figure 6: The ratio of primary to parasitic secondary quantities [32].

with  $R(i)$  and  $L(i)$  being the primary quantities of switching stage  $i$ ,  $R_L(i)$  and  $L_R(i)$  the parasitic secondary quantities and  $R_0$  and  $L_0$  the constant offsets due to connecting cables from the line replica to the matrix. By using the serial impedance as a summary quantity and applying the least absolute deviations (LAD) algorithm according to Eq. (5), an accurate and resource-efficient method to determine a state with the smallest deviation from the nominal values  $R_z$  and  $L_z$  is implemented [32].

$$\min \sum_{i=1}^N \left[ \left| \frac{R_z - R_i}{R_z} \right| + \left| \frac{\omega L_z - \omega L_i}{\omega L_z} \right| \right] \quad (5)$$

Figure 7 presents replication capabilities and operating limits of the transmission line replicas on the basis of four line types according to Table 2. The dot markers in the figure show 500 m intervals of the transmission line. The dashed functions represent corresponding theoretical ideal curves of the transmission line. Reaching the operating limits can be easily recognized by the strong deviation of the transmission line values from the ideal curve.

### 3.3 Software architecture and user-oriented automation system

The following section presents the automation and software solutions that together form the holistic software architecture of the experimental field according to Figure 2.

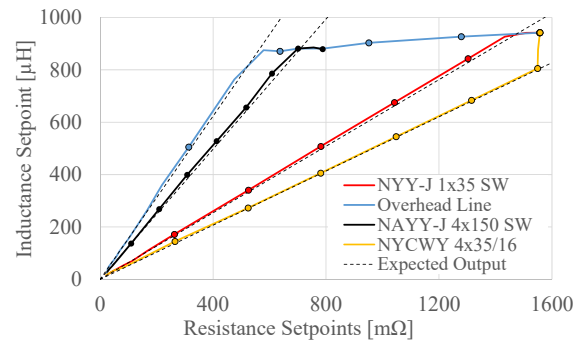


Figure 7: Capabilities and operation limits of TRL replicas [32].

Table 2: Line types under test [32].

Pos.	Line type	$R'$ [m $\Omega$ /km]	$L'$ [ $\mu$ H/km]	$C'$ [nF/km]
i	NYY-J 4 $\times$ 35 SW	524	271	152
ii	NFA2X 1 $\times$ 50 RM	641	995	12
iii	NAYY-J 4 $\times$ 150 SW	206	256	156
iv	NYCWY 4 $\times$ 35/16	524	271	135

### 3.3.1 Supervision system

The supervision system of the busbar matrix based on the Beckhoff TwinCAT-3 platform PLC has the guiding function over the whole experimental field. It is responsible for:

- (i) The logical assignment of the grid participants to the corresponding user for the duration of an experiment. Of course, this only happens if the grid participant is free and the user also has the permissions to use it.
- (ii) Preliminary conformity check. Prior to the execution of the experiment, an attempt is made to identify hazards that could lead to the test being aborted and therefore should be signaled to the user as a warning.<sup>9</sup> Examples of this would be the possibility of violating the permissible power for the component or the permissible busbar current.
- (iii) Monitoring and control of the contactors of the matrix including the feedback contacts as well as the load breaker of the individual components on the point of connection to the busbar matrix. The state change only happens upon valid request from the respective director system, cf. next subsection and Figure 2, and the successful passing of the automatic conformity check of the switching process during runtime. Among other things, it is checked whether the user has the rights for the process, whether the components are available and whether the states of the contactors involved match the expected value.
- (iv) Power monitoring and operational safety management. As mentioned in Section 3.2 the supervision system captures currents and the power of the individual grid participants during runtime. Based on the experiment topology, the current load on the busbars is determined. The laboratory administrator can use the process control center to define the corresponding triggering threshold and triggering delay for the soft current trip. Furthermore, the supervision system monitors the maximum permissible power that the user is allowed to use. If the power is exceeded, the active generators are gradually shedded and the user is informed of this by a message. Additionally, the measuring systems of the busbar matrix are checked cyclically via a live

signal and the states of the circuit breakers within the matrix are monitored.

- (v) Furthermore, events that occur during runtime, such as a circuit breaker trip, are recorded and transmitted to the database by the supervisory system.

To fulfill the tasks, the supervision system interacts with the IO terminals of the busbar matrix and is connected via various interfaces to the four director systems, the power analyzer on grid participants terminal of the matrix, the data management systems, the intermediate services such as ELSA, Tango Controls etc. and the process control center. Communication between the devices is realized according to the request-response method. The datagrams consist of a header of constant length and a dynamic data area. The header contains the control or status information for controlling the data flow of the dynamic data area. The dynamic data area contains data whose meaning is described by the label. Data exchange between the process control center takes place via the TwinCAT Automation Device Specification (ADS) protocol.

### 3.3.2 Director systems

The primary task of the four director systems is to carry out the planned experiments as well as to aggregate the data generated during the experiment and the events that have occurred. For this purpose, each director system performs a process scheduler task, which is responsible for processing the execution sequence according to hard real-time. This is invoked at the beginning of the experiment and remains active until the experiment is completed or a termination condition occurs. The topology and parameters of the experiment as well as the scenario are provided by the data management system, more precisely SupervisionDB. This information is then reflected in the task table of the scheduler. The provision of the experimental microgrid topology of the busbar matrix takes place via the requests to the supervisor system using the EtherCAT-Follower interface. Communication between the director system and the intelligent electronic device of the grid participants also occurs via EtherCAT, but in this case using the EtherCAT-Leader interface. The exchange of data occurs according to the request-response method. For this purpose, a system-wide information transfer protocol has been developed. In principle, the director systems submit function calls and parameters on demand to the IED of the grid participants, which in turn transmit status messages, component parameters, measured values and events that have occurred cyclically with a cycle time of 1 ms to

<sup>9</sup> During the whole workflow, cf. Section 3.4, deviations from expected conditions are detected and reported to the user or lab administrator via the warning and error reporting system of the process control center.

the respective director system. The control commands calls can be initiated either from the scheduler's task table or by the operator's manual intervention via the process control station. Remote monitoring and control via the process control center involves Tango Control Intermediate Services, which is responsible for translating web technology-based control commands from the process control center web client to the ADS protocol used by director system for remote monitoring and control, and vice versa. The upload of measurement data, events and relevant status messages, to the global time series database for post-analysis and archiving (DAQ-DB) is performed via the TwinCAT 3 Database Server.

### 3.3.3 Intelligent electronic devices

A major challenge in heterogeneous power system environments is the integration of the proprietary control systems of the grid participants into the laboratory-wide automation system. The IEDs, equipped with the Generic Component Framework (GCFW) developed specifically for this purpose, provide the required abstraction layer. Drawing on the wide range of Beckhoff PLCs as IEDs as well as various IO terminals and communication interfaces, almost all common power systems can be integrated in terms of hardware. The GCFW is the enabler for consistency of Remote Procedure Calls (RPC) across all supported hardware to ensure both code portability and minimize code duplication. To achieve this, the GCFW implements so-called abstraction functions to translate the generic and plant-wide messages into the component-specific function calls that have to be implemented in the course of component integration. Thus, specific component APIs are accessible via the director system using RPCs according to the unified scheme [33]. In addition, the GCFW implements functionalities for cyclic acquisition and forwarding of all relevant measured data, parameters and component status messages to the director system.

### 3.3.4 Data management systems

In the environment of a fully-automated microgrid laboratory, a large number of different data is generated. For meaningful post-analysis and reproduction of the experiments, it is essential to persist this data clearly assignable. For this purpose, the SESCL is equipped with various databases, which meet the respective requirements, whereby three key databases are to be explicitly emphasized here. SupervisionDB is an object-relational database, which is responsible for the handling of all

administrative data, the master data of the experimental field and the components as well as the metadata of the experiments. The management of the time series descriptors for unambiguous assignment of the time series of measurements to respective components and experiments is also subject to this database. In turn, ELSA-DB and DAQ-DB are time series databases and are responsible for data management of the collected measurements. As described in the Section 3.2, ELSA-DB is responsible for data storage of the high-frequency raw values of the power analyzer and the DAQ-DB is used to handle all other measured values and events provided by director systems, intelligent electronic devices, the process control center or the measuring equipment.

### 3.3.5 Intermediate services

The usage of intermediate services based on open source solutions, see Figure 2, is motivated by the desire to reduce the overall complexity and the required performance of the systems. This approach follows the Unix philosophy of decentralizing the solution of various tasks so that each of the parts is given more autonomy and specialization in accomplishing a corresponding task [34]. This has the following essential consequences: optimization of resource sharing, increase of reliability and availability, reduction of processing time by concurrency. This principle and its consequences are illustrated in concrete terms by the intermediate services running in SESCL. As mentioned in Section 3.2, ELSA is responsible for the acquisition, archiving and visualization of current and voltage raw values of the power analyzer with time resolution of 50  $\mu$ s. The system architecture consists of a time series database, a visualization application and the measurement acquisition service. Each subcomponent is specialized for one task and is operated autonomously from the others. Concurrently with ELSA, the Telegraf server agent also accesses the power analyzers and transmits low-frequency (200 ms) data that has already been preprocessed by the internal DSP, such as power, RMS voltage, etc., to the DAQ-DB for logging and to Grafana based dashboards for live-value monitoring in Process Control Center.

In the SESCL context it is extremely important for the interpretation of the results that the measured values can be assigned to each other exactly in time. For this purpose EtherCAT devices and system measurement equipment implement a high precision time synchronization facility based on the IEEE-1588 Precision Time Protocol (PTP). The Grandmaster Clock intermediate services provides the correspondingly precise reference clock on the basis of which all other devices are subsequently synchronized.

Thus, data with a time accuracy of up to 1  $\mu$ s can be provided.

Further intermediate services in the SESCL environment are Tango Controls<sup>10</sup> to provide web technologies based HMI for monitoring and control of experiments, Grafana<sup>11</sup> the open source platform for analysis and visualization of collected data and Eclipse Mosquitto<sup>12</sup> as a MQTT broker.

### 3.3.6 Process control center

The process control center (PCC) provides a consistent interface for user and resource management, experiment scheduling and execution as well as visualization of the topology and relevant system and component parameters with the ability to monitor and control participants and topology. The interface can be divided into three spaces:

The administration space is only available to the lab administrator. Here, users and groups are administered, resources are managed, system parameters are defined, and the permissible currents of the busbars and the power released for user groups are specified. During runtime, the lab administrator can observe the system information and

states provided by the supervision system in real time and abort the experiment if necessary. Errors that lead to the triggering of the safety precautions implemented in the hardware can also only be acknowledged in this domain.

In the customer space, new experiments can be created and existing ones can be managed. In the topology panel, the user can define the desired experiment topology from the authorized resources. On the scheduling panel, the user defines the experiment procedure using the RPCs of the grid participants and busbar matrix. The record panel allows to select the acquisition values to be stored in the database.

The third space of the PCC, the monitoring and control client based on web technologies, is also accessible from the customer space. In this space, the topology of the experiment is displayed graphically and the execution sequence of the experiment is presented with the highlighting of the current step. It allows to change the position of the participants according to the wishes and to save or load the resulting layout. From this screen the experiment can be started and stopped, cf. Figure 8. At runtime, the user can use the web client to observe the live-values almost in real time and intervene to remote control the grid participant and the connection between them. With a right click on the component or busbar, a corresponding Grafana or ELSA based dashboard configurable by user can be opened, which graphically displays the chosen live values. After

<sup>10</sup> <https://www.tango-controls.org/>.

<sup>11</sup> <https://grafana.com/>.

<sup>12</sup> <https://mosquitto.org/>.

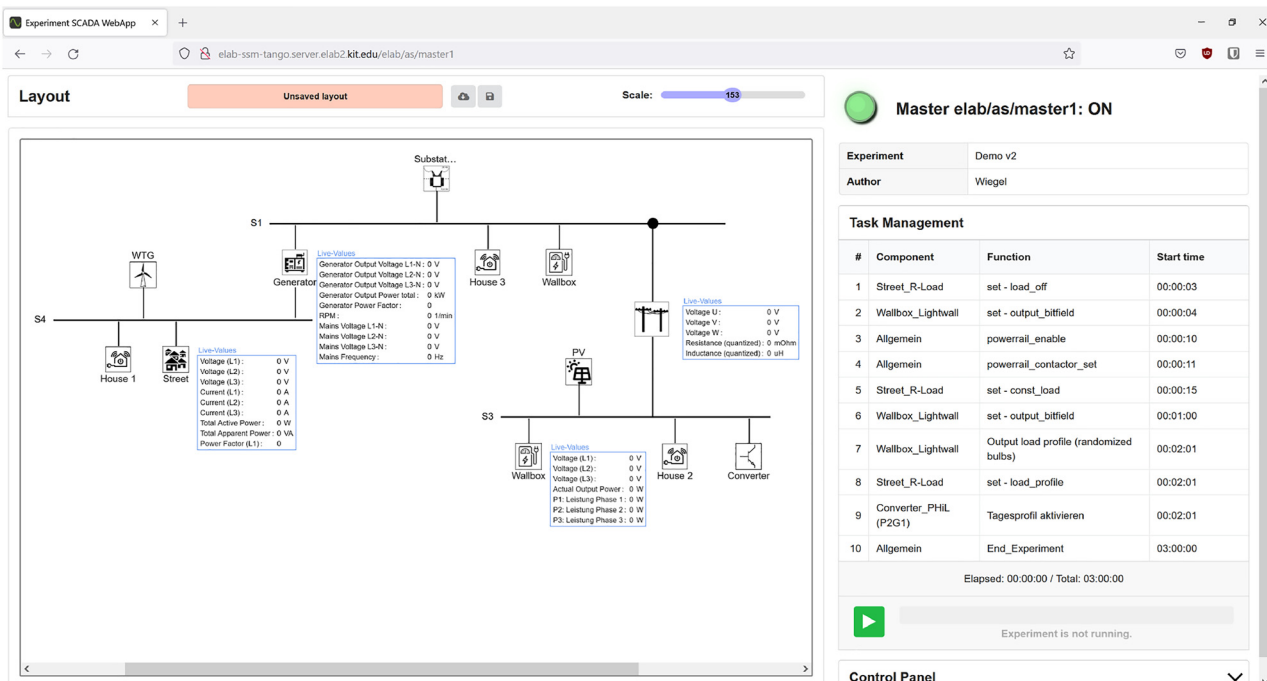
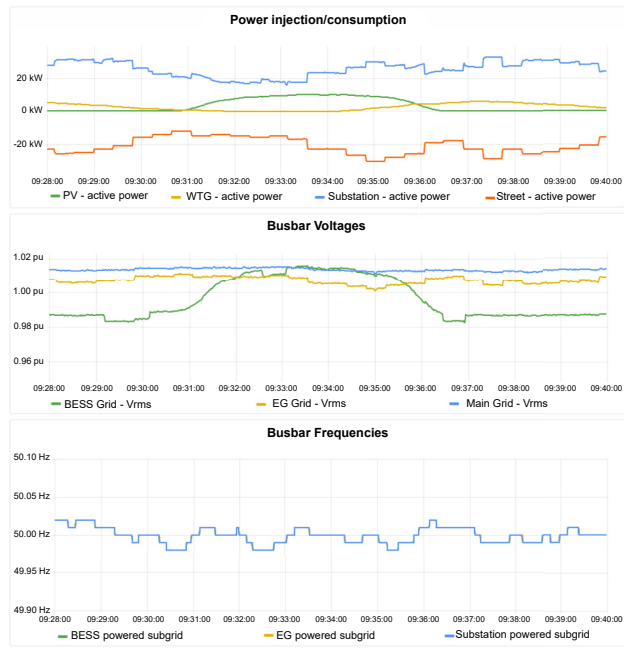
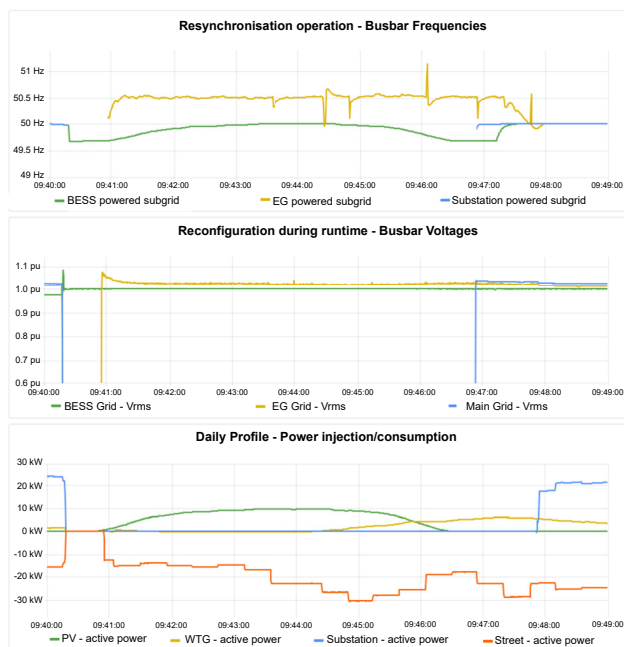


Figure 8: Setup of use case in the web client of the process control center.

the completion of the experiment, the values desired for closer examination can be chosen from the parameter list. The values are plotted over the duration of the experiment and the user has the option to zoom into the desired time interval, cf. Figures 9 and 10.



**Figure 9:** Daily profiles of consumption as well as renewable energy injection, visualized in the process control center.



**Figure 10:** Blackout and resynchronization, visualized in the process control center.

To perform the described tasks, the process control center interacts with various elements of the overall SESCL architecture. System monitoring is performed via a direct ADS connection to the supervision system. For administration, user and resource management it is equipped with an interface to the databases of the data management system. The runtime monitoring and control is done by including the intermediate services. Tango-Controls serves as the back-end for providing the various interfaces to the director systems. The Grafana based dashboards are integrated with the iframe functionality of HTML. Live values from the power analyzers are streamed from Telegraf agent via an HTTP REST API.

### 3.4 Workflow

The experimental procedure is divided into the following phases: During the organization phase, the lab administrator first assigns resources to the user. In the planning phase, the user first logs in on customer space of the PCC with valid credentials. In the background, the user is assigned one of the director systems for the session. Then the experiment name is specified, the desired grid participants are selected and the corresponding microgrid topology is defined. In the scheduler, the user determines the script of the experiment, using the available predefined functions of the components and the matrix. At the same time, the user can call up the monitoring and control client based on web technologies and specify which parameters he wants to observe as live values and which should be logged in the database. Then the following series of steps run in the background, unnoticed by the user, before the test can be started: (i) Validity check. A trivial preliminary check of the power equilibrium is carried out:  $P_p \geq |P_C - P_G|$ . The difference in power of all generators  $P_G$  and all consumers  $P_C$  must not be greater than the power of the prosumers  $P_p$ . Users with extended rights can skip this check. (ii) The supervision system receives the information regarding the topology and the planned test procedure. (iii) Based on this information the EtherCAT patchfield is configured in such a way that the director system can communicate with all IEDs of the participants. (iv) Corresponding structures are created in the databases and time series descriptors are generated, which then refer to the corresponding time range of the measurement parameters. (v) If all requirements are met, the experiment is started. At runtime, the user can use the web client to observe the experiment live with a slight delay and intervene to control it. After the experiment is completed, the user can view the historical data and perform post-analysis.

## 4 Use case: islanding capabilities of BESS and EG

SESCL has already been used for various use cases. Including research activities such as experimental validation of energy packet-based dispatching algorithms [35], development and field assessment of the function and usability of a smart charging application [36], and evaluation of an adaptive feedforward control algorithm for DC/DC converters in microgrids as a PHIL study [37]. The following section presents a further use case to illustrate the capabilities of the SESCL research infrastructure.

### 4.1 Setup and scenario

The current use case demonstrates the islanding capability of a conventional emergency generator (EG) and a modern battery energy storage system (BESS). Furthermore, this configuration proves that the presented laboratory is able to automatically set up an experimental microgrid with given parameters that can be modified during runtime both in terms of setpoint (e.g., load behavior/profile) and topology (adding or removing components during the experiment runtime), while remaining in a safe and operational state.

The grid topology of a small Mediterranean island, corresponding to Figure 8, is reproduced. The grid consists of three nodes which are referred to as busbars to account for the hardware representation. During nominal operation, all three busbars are energized by the substation which represents the connection point to the public grid via a submarine cable and all DER units operate in grid following/supporting mode [38] according to the local objective, such as maximum power injection (wind turbine generator and PV) or PQ-controlled (BESS). Then, an emulated fault in the grid leads to a blackout of the substation and a separation of the transmission line which connects busbar S1 and busbar S3. These two events are coordinated by the automation system. The incident is detected by both the conventional gas powered emergency power supply of S4 and the BESS of S3. Due to the synchronous nature of the BESS providing grid services, it can seamlessly switch from grid supporting to grid forming mode and power the busbar without interruption. Meanwhile start-up procedure of the conventional gas generator powering busbar S4 leads to a power interruption. After the restoration of the connection

to public grid both subgrids resynchronize with the main grid.

### 4.2 Experimental results and discussion

This section presents the results of the experiment described in Section 4.1. Figure 9 shows the behavior of the system during nominal operation, in the top plot the daily profiles of selected components are shown. The timescale for an emulated day is set to 10 min, after which the profile is repeated if no other command is given. The corresponding busbar RMS voltages are presented in the middle plot, as expected the voltages drop over the cable length. Busbar S4 is connected via roughly 50 m of cable NAYY-J 4 × 50 SW and busbar S3 is connected via a transmission line replica corresponding to 500 m of NAYY-J 4 × 70 SW. Since the busbars are connected, the frequencies match very closely as can be seen in the lower plot of Figure 9.

The described blackout and resynchronization is presented in Figure 10. In the middle plot, the sudden voltage drop of busbar S1 and S3 can be clearly seen, whereas the voltage of busbar S4 only experiences minor disturbances due to switching to grid forming mode of the BESS. The frequency droop behavior of the BESS is shown in the upper plot. After the sudden drop in frequency due to the necessary increase in power injection, the frequency recovers based on the power injection of the connected PV system, as seen in the lower plot.

During the start-up phase of the gas powered emergency system, S4 remains in blackout state. After the start of the generator, the subgrid is energized and can resume normal operation, but with limited service quality as is evident by the large frequency deviation.

After the return of the substation, the BESS as well as the gas generator commence resynchronization in preparation of reconnecting to the main grid as can be seen in the upper plot of Figure 10. To better illustrate the timescale of the resynchronization, the PLL angles of the BESS system as well as the substation grid during the resynchronization process are shown in Figure 11. The process is completed within 0.4 s using an PI-control based active synchronization approach [39].

From the presented results it can be concluded that a reconfiguration of the microgrid topology under study is possible with the hardware setup of the SESCL, which offers a reliable and reproducible infrastructure to tackle the challenges posed by the integration of DER units as well as a changing grid topology.

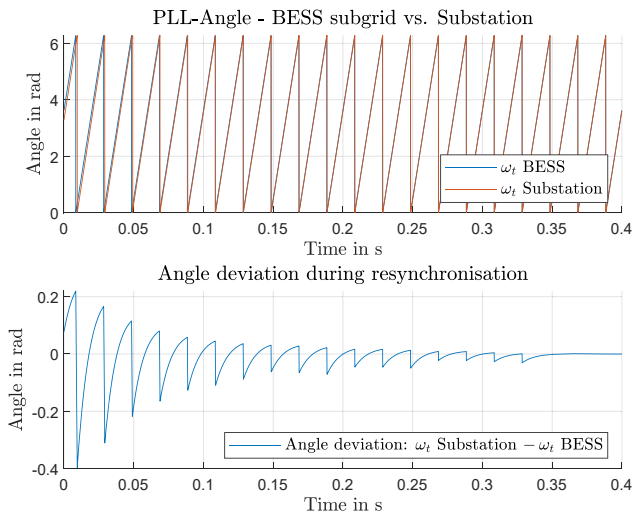


Figure 11: BESS resynchronization process.

## 5 Conclusion and future work

In the present article, we introduce the Smart Energy System Control Laboratory (SESCL) as a fully-automated and user-oriented research infrastructure for controlling and operating smart energy systems in the context of a microgrid-under-test setting. The goal of SESCL is to model, control and experimentally validate new energy technologies. The concept and specifications of SESCL are detailed in the light of numerous European Smart Grid Laboratories.

The key advantages of our approach are the following:

(i) the provisioning of a fully-automated busbar matrix to provide a very flexible and adjustable microgrid topology; (ii) the capability of load shedding or integration of grid participants, as well as changing the microgrid topology on demand; (iii) and the possibility to control and modify setpoints and operating parameters of grid participants during runtime. A specific use case – islanding of a microgrid – is utilized to illustrate the capabilities of the SESCL research infrastructure. Concluding, the synergy of the harmonized hardware and software solutions of SESCL provides a well-organized workflow for the planning, safe execution and analysis of experiments for the modeling of future energy systems and microgrids with variable topology.

Part of the ongoing work is to test and evaluate a recently deployed high-performance, low-latency interface between the Opal-RT real-time simulator in SESCL and the RTDS-based real-time simulation cluster in the Energy

Grids Simulation and Analysis Laboratory<sup>13</sup> (EGSAL) of Energy Lab 2.0 in terms of closed-loop delay and the resulting effects on simulation accuracy. In one of the following scenarios, the RTDS simulator cluster will be used to simulate a detailed model of the KIT North Campus 20 kV [40] power grid, and the SESCL experimental microgrid will be connected to the simulated power grid via the power hardware-in-the-loop facility. This setup will provide a foundation for testing new power grid solutions, both from the software and hardware perspectives, using the Energy Lab 2.0 infrastructure.

**Acknowledgement:** We thank Tobias Moser for editing the illustrations.

**Author contributions:** Author contributions according to Contributor Roles Taxonomy (CRediT, <https://www.casrai.org/credit.html>): *Conceptualization:* F.W.; *Investigation:* F.W., J.W.; *Writing – original draft:* F.W., J.W. and M.K.; *Writing – review and editing:* F.W., J.W., M.K., R.M., S.W., V.H.; *Visualization:* F.W.; *Supervision:* S.W., V.H.; *Project administration:* F.W.; *Funding acquisition:* V.H.

**Research funding:** The Energy Lab 2.0 and thus also the Smart Energy System Control Laboratory was funded by the Helmholtz Association, the German Federal Ministry of Education and Research (BMBF), and the Ministry of Science, Research and Art (MWK) of the State of Baden-Wuerttemberg.

**Conflict of interest statement:** The authors declare no conflicts of interest regarding this article.

## References

- [1] M. Z. Jacobson, M. A. Delucchi, M. A. Cameron, et al., “Impacts of green new deal energy plans on grid stability, costs, jobs, health, and climate in 143 countries,” *One Earth*, vol. 1, no. 4, pp. 449–463, 2019.
- [2] T. Brown, T. Bischof-Niemz, K. Blok, C. Breyer, H. Lund, and B. Mathiesen, “Response to ‘burden of proof: a comprehensive review of the feasibility of 100% renewable-electricity systems,” *Renewable Sustainable Energy Rev.*, vol. 92, pp. 834–847, 2018.
- [3] J. Peter and J. Wagner, “Optimal allocation of variable renewable energy considering contributions to security of supply,” *Energy J.*, vol. 42, no. 1, pp. 229–259, 2021.
- [4] R. Shankar and P. Kundur, *Power System Stability and Control*, New York, McGraw-Hill Books, 1994.
- [5] M. Liserre, T. Sauter, and J. Y. Hung, “Future energy systems: integrating renewable energy sources into the smart power

<sup>13</sup> <https://www.iai.kit.edu/english/RPE-EGSAL.php>.

- grid through industrial electronics,” *IEEE Ind. Electron. Mag.*, vol. 4, no. 1, pp. 18–37, 2010.
- [6] G. Spagnuolo, G. Petrone, S. V. Araujo, et al., “Renewable energy operation and conversion schemes: a summary of discussions during the seminar on renewable energy systems,” *IEEE Ind. Electron. Mag.*, vol. 4, no. 1, pp. 38–51, 2010.
- [7] W. Winter, K. Elkington, G. Bareux, and J. Kostevc, “Pushing the limits: Europe’s new grid: innovative tools to combat transmission bottlenecks and reduced inertia,” *IEEE Power Electron. Mag.*, vol. 13, no. 1, pp. 60–74, 2014.
- [8] B. M. Buchholz and Z. Styczynski, *Smart Grids-Fundamentals and Technologies in Electricity Networks*, vol. 396, Heidelberg, Springer, 2014.
- [9] T. Strasser, F. Andren, J. Kathan, et al., “A review of architectures and concepts for intelligence in future electric energy systems,” *IEEE Trans. Ind. Electron.*, vol. 62, no. 4, pp. 2424–2438, 2015.
- [10] X. Yu, C. Cecati, T. Dillon, and M. G. Simões, “The new Frontier of smart grids,” *IEEE Ind. Electron. Mag.*, vol. 5, no. 3, pp. 49–63, 2011.
- [11] C. Cecati, G. Hancke, P. Palensky, P. Siano, and X. Yu, “Guest editorial special section on information technologies in smart grids,” *IEEE Trans. Ind. Inform.*, vol. 9, no. 3, pp. 1380–1383, 2013.
- [12] V. C. Gungor, D. Sahin, T. Kocak, et al., “Smart grid technologies: communication technologies and standards,” *IEEE Trans. Ind. Inform.*, vol. 7, no. 4, pp. 529–539, 2011.
- [13] P. Pourbeik, P. Kundur, and C. Taylor, “The anatomy of a power grid blackout – root causes and dynamics of recent major blackouts,” *IEEE Power Electron. Mag.*, vol. 4, no. 5, pp. 22–29, 2006.
- [14] G. Notton, M. L. Nivet, D. Zafirakis, F. Motte, C. Voyant, and A. Fouilloy, “Tilos, the first autonomous renewable green island in Mediterranean: a Horizon 2020 project,” in *2017 15th International Conference on Electrical Machines, Drives and Power Systems (ELMA)*, 2017, pp. 102–105.
- [15] T. Strasser, F. P. Andrén, G. Lauss, et al., “Towards holistic power distribution system validation and testing—an overview and discussion of different possibilities,” *Elektrotech. Inf.*, vol. 134, no. 1, pp. 71–77, 2016.
- [16] R. Awasthy, S. Flint, R. Sankaranarayana, and R. L. Jones, “Bridging the gap – a workshop of industry practitioners and university researchers,” in *TENCON 2017 – 2017 IEEE Region 10 Conference*, 2017, pp. 2504–2509.
- [17] V. Hagenmeyer, H. K. Cakmak, C. Döpmeier, et al., “Information and communication technology in Energy Lab 2.0: smart energies system simulation and control center with an Open-Street-Map-based power flow simulation example,” *Energy Technol.*, vol. 4, pp. 145–162, 2016.
- [18] N. Hatziaargyriou, J. Milanovic, C. Rahmann, et al., “Definition and classification of power system stability – revisited & extended,” *IEEE Trans. Power Syst.*, vol. 36, no. 4, pp. 3271–3281, 2021.
- [19] L. L. Jansen, N. Andreadou, I. Papaioannou, and A. Marinopoulos, “Smart grid lab research in Europe and beyond,” *Int. J. Energy Res.*, vol. 44, no. 3, pp. 1307–1336, 2020.
- [20] N. Andreadou, L. Jansen, A. Marinopoulos, and I. Papaioannou, *Smart Grid Laboratories Inventory 2018*, Luxembourg, Publications Office of the European Union, 2019.
- [21] R. Brundlinger, T. Strasser, G. Lauss, et al., “Lab tests: verifying that smart grid power converters are truly smart,” *IEEE Power Electron. Mag.*, vol. 13, no. 2, pp. 30–42, 2015.
- [22] O. B. Fosso, M. Molinas, K. Sand, and G. H. Coldevin, “Moving towards the smart grid: the Norwegian case,” in *2014 International Power Electronics Conference (IPEC-Hiroshima 2014 – ECCE ASIA)*, 2014, pp. 1861–1867.
- [23] SINTEF. (n.d.). *Smart Grid Laboratory*. Retrieved from <https://www.sintef.no/en/all-laboratories/smartgridlaboratory>.
- [24] A. Spina, K. Rauma, C. Aldejohann, et al., “Smart grid technology lab – a full-scale low voltage research facility at TU Dortmund university,” in *2018 AEIT International Annual Conference*, 2018, pp. 1–6.
- [25] N. Hadjsaid, R. Caire, and B. Raison, “Decentralized operating modes for electrical distribution systems with distributed energy resources,” in *2009 IEEE Power Energy Society General Meeting*, Calgary, Canada, IEEE, 2009, pp. 1–4. Available at: <https://hal.archives-ouvertes.fr/hal-00417650>.
- [26] M. C. Alvarez-Herault, A. Labonne, S. Touré, et al., “An original smart-grids test bed to teach feeder automation functions in a distribution grid,” *IEEE Trans. Power Syst.*, vol. 33, no. 1, pp. 373–385, 2018.
- [27] M. S. Kemal, L. Petersen, F. Iov, and R. L. Olsen, “A real-time open access platform towards proof of concept for smart grid applications,” *J. Commun. Navig. Sens. Serv.*, vol. 2017, no. 1, pp. 49–74, 2018.
- [28] R. E. Mackiewicz, “Overview of IEC 61850 and benefits,” in *2006 IEEE PES Power Systems Conference and Exposition*, IEEE, 2006, pp. 623–630.
- [29] S. Sanchez-Acevedo and S. D’Arco, “Towards a versatile cyber physical power system testbed: design and operation experience,” in *2021 IEEE PES Innovative Smart Grid Technologies Europe (ISGT Europe)*, Institute of Electrical and Electronics Engineers Inc., 2021, pp. 1–6.
- [30] Dena, “Momentanreserve 2030,” Deutsche Energie-Agentur GmbH, Tech. Rep., 2016.
- [31] F. Huerta, J. K. Gruber, M. Prodanovic, and P. Matatagai, “Power-hardware-in-the-loop test beds: evaluation tools for grid integration of distributed energy resources,” *IEEE Ind. Appl. Mag.*, vol. 22, no. 2, pp. 18–26, 2016.
- [32] T. Moser, “Inbetriebnahme und betriebsverhaltensanalyse einer parametrisierbaren leitungs nachbildung für niederspannungsverteilstetze,” Bachelor thesis, DHBW, Karlsruhe, 2020.
- [33] A. D. Birrell and B. J. Nelson, “Implementing remote procedure calls,” *ACM Trans. Comput. Syst.*, vol. 2, no. 1, pp. 39–59, 1984.



- [34] E. S. Raymond, *The Art of UNIX Programming*, Boston, Pearson Education, 2003.
- [35] F. Wiegel, E. De Din, A. Monti, et al., “A novel receiver design for energy packet-based dispatching,” *Energy Technol.*, vol. 9, no. 2, p. 2000937, 2021.
- [36] S. Meisenbacher, K. Schwenk, J. Galenzowski, S. Waczowicz, R. Mikut, and V. Hagenmeyer, “A lightweight user interface for smart charging of electric vehicles: a real-world application,” in *2021 9th International Conference on Smart Grid and Clean Energy Technologies (ICSGCE)*, 2021, pp. 57–61.
- [37] J. Wachter, L. Gröll, and V. Hagenmeyer, “Adaptive feedforward control for dc/dc converters in microgrids – a power hardware in the loop study,” in *2021 9th International Conference on Smart Grid (icSmartGrid)*, 2021, pp. 49–56.
- [38] J. Rocabert, A. Luna, F. Blaabjerg, and P. Rodríguez, “Control of power converters in AC microgrids,” *IEEE Trans. Power Syst.*, vol. 27, no. 11, pp. 4734–4749, 2012.
- [39] C. Cho, J. H. Jeon, J. Y. Kim, S. Kwon, K. Park, and S. Kim, “Active synchronizing control of a microgrid,” *IEEE Trans. Power Syst.*, vol. 26, no. 12, pp. 3707–3719, 2011.
- [40] M. Weber, M. Kyesswa, U. Kühnapfel, V. Hagenmeyer, and H. K. Çakmak, “Case study of designing a locally distributed real-time simulation infrastructure,” in *2021 IEEE Electrical Power and Energy Conference (EPEC)*, 2021, pp. 310–315.



Jan Wachter (M.Sc.) is a research associate at the Research Platform Energy department at the Institute for Automation and Applied Informatics at the Karlsruhe Institute of Technology pursuing a Ph.D. in mechanical engineering. Main research interests: control of power electronic devices in microgrids, control of microgrids and sector coupling.



Dr.-Ing. Michael Kyesswa is head of the Energy Grids Simulation and Analysis Laboratory of the Research Platform Energy department at the Institute for Automation and Applied Informatics, Karlsruhe Institute of Technology. Main areas of research: Modelling, simulation and analysis of power systems, parallel and real-time simulations, and computational methods for power system analysis.

## Bionotes



Friedrich Wiegel (M.Sc.) leads the Smart Energy System Control Laboratory at the Institute for Automation and Applied Informatics at the Karlsruhe Institute of Technology while pursuing a Ph.D. in electrical engineering. His research interests include power system modeling, microgrid operation and automation, information and communication technology for power systems, and power hardware in the loop.



Ralf Mikut received the Ph.D. and Habilitation degrees in mechanical engineering from the University of Karlsruhe in 1999 and 2007, respectively. Since 2011, he has been an Adjunct Professor at the Faculty of Mechanical Engineering and the Head of the Research Group “Automated Image and Data Analysis,” Institute for Automation and Applied Informatics at Karlsruhe Institute of Technology. His current research interests include machine learning, data analytics, image processing, life science applications, and smart grids.



Dr.-Ing. Simon Waczowicz heads the Research Platform Energy department at the Institute for Automation and Applied Informatics at the Karlsruhe Institute of Technology. Main research interests: Energy system modeling, time series analysis and forecasting, energy management, sector coupling.



Veit Hagenmeyer received the Ph.D. degree from Université Paris XI, Paris, France, in 2002. He is currently a Professor of Energy Informatics with the Faculty of Computer Science, and the Director of the Institute for Automation and Applied Informatics, Karlsruhe Institute of Technology, Karlsruhe, Germany. His research interests include modeling, optimization and control of sector-integrated energy systems.